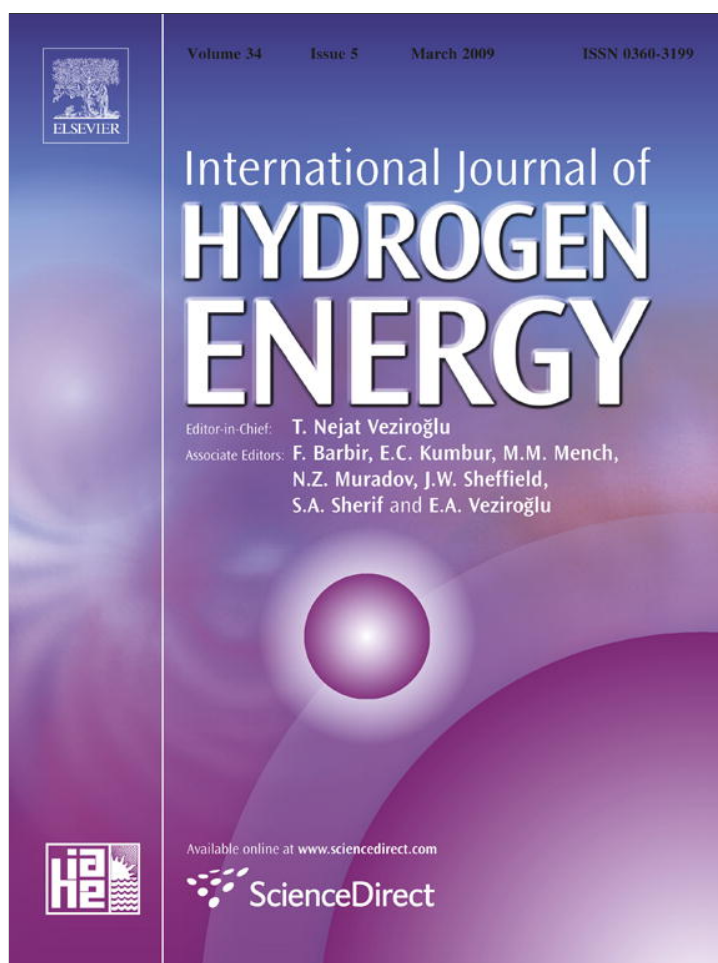


Provided for non-commercial research and education use.
Not for reproduction, distribution or commercial use.

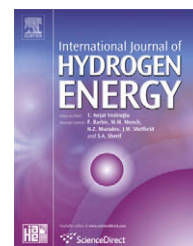


This article appeared in a journal published by Elsevier. The attached copy is furnished to the author for internal non-commercial research and education use, including for instruction at the authors institution and sharing with colleagues.

Other uses, including reproduction and distribution, or selling or licensing copies, or posting to personal, institutional or third party websites are prohibited.

In most cases authors are permitted to post their version of the article (e.g. in Word or Tex form) to their personal website or institutional repository. Authors requiring further information regarding Elsevier's archiving and manuscript policies are encouraged to visit:

<http://www.elsevier.com/copyright>

Available at www.sciencedirect.comjournal homepage: www.elsevier.com/locate/he

Stability improvements of Ni/ α -Al₂O₃ catalysts to obtain hydrogen from methane reforming

Francisco Pompeo^{a,b}, Delia Gazzoli^c, Nora N. Nichio^{a,b,*}

^aCINDECA, Facultad de Ciencias Exactas, Universidad Nacional de La Plata, CONICET, 47 N° 257, 1900 La Plata, Argentina

^bFacultad de Ingeniería, Universidad Nacional de La Plata, 1 esq. 47, 1900 La Plata, Argentina

^cDipartimento di Chimica, Università di Roma "La Sapienza", P.le A. Moro 5, 00185 Rome, Italy

ARTICLE INFO

Article history:

Received 26 November 2008

Received in revised form

19 December 2008

Accepted 19 December 2008

Available online 30 January 2009

Keywords:

Hydrogen

Nickel

α -Al₂O₃

Ce_xZr_{1-x}O₂ mixed oxide

XPS

ABSTRACT

Ni catalysts supported on commercial α -Al₂O₃ modified by addition of CeO₂ and/or ZrO₂ were prepared in the present work. Since the principal objective was to evaluate the behavior of these systems and the support effect on the stability, methane reforming reactions were studied with steam, carbon dioxide, partial oxidation and mixed reforming. Results show that catalysts supported on Ce–Zr– α -Al₂O₃ composites present better reforming activity and stability noticeably higher than in the case of the reference support. With respect to composites, the presence of mixed oxides of Ce_xZr_{1-x}O₂ type facilitates the formation of active phases with higher interaction. This fact reduces the deactivation by sintering conferring to the system a higher contribution of adsorbed oxygen species, favoring the deposited carbon elimination. These improvements resulted in being dependent on the Ce:Zr ratio of the composite, thus obtaining more stable catalysts for Ce:Zr = 4:1 ratios.

© 2009 International Association for Hydrogen Energy. Published by Elsevier Ltd. All rights reserved.

1. Introduction

In the near future, we will find an important increase of hydrogen demand, which will be affected not only by applications in ammonium production, Fischer–Tropsch synthesis, processes in oil refineries and chemical industries, but also by the use of hydrogen in fuel cells [1–4]. Therefore, it is still interesting for R&D groups to continue with the study of processes for procurement of synthesis gas (CO and H₂) from natural gas using different reforming agents such as H₂O, O₂, CO₂, H₂O and O₂, and the development of catalysts that minimize the energetic requirement [5].

Supported Ni catalysts have resulted in being important due to comparative costs with precious metals, and to the

excellent activity reported in reforming reactions. However, the particular problem is the strong deactivation by carbon deposition, which induces the search of modifications in the catalyst formulation and in selection of operative conditions to improve this aspect [6–8].

The support role on the stability of catalysts is well known. Although α -Al₂O₃ is an adequate support for reforming processes by its chemical and physical stability and mechanical strength, it presents the disadvantage that by its low reactivity it leads to a weak interaction metal-support with the active phase. In this sense, this research group has performed works oriented to modify the alumina by the addition of an aluminum oxide layer, facilitating a higher interaction with the metal and decreasing the sintering of the

* Corresponding author. CINDECA, Facultad de Ciencias Exactas, Universidad Nacional de La Plata, CONICET, 47 N° 257, 1900 La Plata, Argentina.

E-mail address: nnichio@quimica.unlp.edu.ar (N.N. Nichio).

0360-3199/\$ – see front matter © 2009 International Association for Hydrogen Energy. Published by Elsevier Ltd. All rights reserved.
doi:10.1016/j.ijhydene.2008.12.057

active phase [9]. We have also used alkaline metals with marked Lewis basicity such as Li or K, which allowed a noticeable reduction in carbon deposition [10].

On the other hand, pure CeO₂, ZrO₂ and CeO₂-ZrO₂ supports were also used for favoring carbon gasification due to their oxygen storage capacity (OSC) [11,12]. The high cost of these supports makes them difficult to be applied in commercial formulations. For this reason, some proposals have been made including the addition of CeO₂ on γ -Al₂O₃ for dry reforming [13], Ce-ZrO₂ on θ -Al₂O₃ for steam and oxy-steam reforming [14,15], CeO₂-ZrO₂ on γ -Al₂O₃ for partial oxidation of methane [16,17], and CeO₂-ZrO₂ on SiO₂ for auto-thermal reforming [18]. In all these works, starting supports have surface area values higher than 160 m² g⁻¹, and authors reported important improvements in the catalyst stability attributed to modification of supports.

In order to obtain an efficient Ni-containing catalyst supported on α -Al₂O₃ that has a surface area lower than 10 m² g⁻¹, we have prepared and characterized Ce-Zr- α -Al₂O₃ composites. Our results demonstrate that the excellent refractory properties of α -Al₂O₃ are maintained and the presence of patches of mixed oxides of the type Ce_{1-x}Zr_xO₂ on the catalyst surface increases sites with strong basic nature [19].

The present work evaluates the fundamental catalytic properties of Ni systems supported on Ce-Zr- α -Al₂O₃ in different reforming reactions (partial oxidation (POM), steam reforming (SR), mixed reforming (MR) and dry reforming (DR)).

Special attention has been devoted to the study of the catalyst stability facing severe deactivation conditions to evaluate the support effect.

2. Experimental

Commercial α -Al₂O₃ Rhone Poulenc (Spheralite 512; surface area around 10 m² g⁻¹) was used as base support. Modified supports were prepared by successive impregnations of α -Al₂O₃ first with ZrO(NO₃)₂ · xH₂O (Aldrich), and then with Ce(NO₃)₃ · 6H₂O (Alpha) aqueous solutions. They were dried at 120 °C for 12 h and calcined in air for 4 h at 600 °C. The supports are designated as xCe_yZr_z α , where x and y represent the % wt/wt of CeO₂ and ZrO₂ respectively and α the α -Al₂O₃ support. The Ni impregnation was carried out with an Ni(NO₃)₂ · 6H₂O (Aldrich) aqueous solution to reach a final

metallic content of 2 wt/wt%. After drying at 120 °C for 12 h the samples were calcined in air flow at 750 °C for 4 h.

In preliminary experiments it was determined that the intraphase transport of mass does not affect the reaction rate when the pellet size of the catalyst is between 0.495 and 0.104 mm. Similarly, the minimum feed flow rate (corresponding to GHSV: 3.1×10^5 cm³ g⁻¹ h⁻¹), above which interphase transport resistances were minimized, was also determined following standard procedures at 700 °C [20].

Partial oxidation (POM), steam reforming (SR), mixed reforming (MR) and dry reforming (DR) reactions were studied in an experimental apparatus in continuous flow, at atmospheric pressure, in the temperature range 400–700 °C and GHSV = 3×10^5 cm³ h⁻¹ g⁻¹. The composition of the feed mixtures was: POM, N₂/CH₄/O₂ = 10/2/1; SR N₂/CH₄/H₂O = 10/2/2; MR, N₂/CH₄/H₂O/O₂ = 10/2/1/1; DR, N₂/CH₄/CO₂ = 6/1/1; (partial pressure of CH₄ ~0.15 bar and C/O ~1).

The catalyst sample used was 0.025 g and the pellet size between 0.12 and 0.15 mm. The catalyst bed was diluted with 0.200 g of α -Al₂O₃ to avoid the development of hot points in particular for POM reaction. Samples were reduced at 700 °C (10 °C min⁻¹) for 1 h in pure H₂ flow (30 cm³ min⁻¹) before catalytic runs. The analysis of reaction products was performed with a gas chromatograph Shimadzu GC-8A equipped with a column HayeSep D 100 and a detector of thermal conductivity.

Two tests were carried out to determine the catalyst stability under different reaction conditions. The sintering of the active phase and the carbon deposition were evaluated according to conditions of Tests (A) and (B) respectively. Test (A) consisted in the SR reaction at 700 °C. After 1 h reaction, the initial activity was determined. The sample was subsequently exposed to water steam and hydrogen flow at 800 °C for 2 h and the activity was then measured under the SR condition at 700 °C. Test (B) consisted in the DR reaction at 700 °C for about 72 h. The stability was evaluated in terms of the activity coefficient a_{CH_4} , which represents the ratio between the CH₄ consumption rate at time t (hours) and the initial rate.

Mean particle size was determined by TEM and obtained in a TEM JEOL 100 C instrument. A graphite pattern was used for calibration. Histograms of particle size distribution arise from microphotographs using the technique of clear field image. The mean diameter of particles was obtained from the second distribution moment named diameter volume-area (d_{va}).

Table 1 – Particle diameter obtained by TEM, metallic dispersion determined by hydrogen chemisorption and from Brunelle equation [22] and hydrogen consumption from TPR analysis.

Catalyst	TEM		H ₂ chemisorption			TPR	
	Average particle diameter (nm) d_{va}	Metal dispersion ^a (%)	Metal dispersion (%)	Metal surface area (m ² g ⁻¹)	H ₂ consumption (mmol H ₂ g ⁻¹)	Reducibility (%)	
Ni α	18	4.7	2.3	0.32	0.27	80	
Ni5Ce α	14	6.0	5.6	0.77	0.22	63	
Ni4Ce1Zr α	12	7.0	7.0	0.95	0.25	74	
Ni2.5Ce2.5Zr α	12	7.0	7.2	0.98	0.19	58	
Ni1Ce4Zr α	14	6.0	5.7	0.78	0.24	69	
Ni5Zr α	16	5.0	5.4	0.75	0.21	62	

a From Brunelle equation [22].

Hydrogen chemisorption measurements were carried out in dynamic equipment with a TCD detector. Samples were reduced in H_2 at $700\text{ }^\circ\text{C}$ for 1 h, cooled in hydrogen up to $400\text{ }^\circ\text{C}$, flushed with argon for 2 h at $400\text{ }^\circ\text{C}$ and then cooled up to room temperature in argon flow. Hydrogen pulses were then injected up to saturation. Dispersions were estimated from the hydrogen amount consumed, assuming an adsorption stoichiometry $H/Ni = 1$.

Tests of temperature programmed reduction (TPR) were carried out in a dynamic conventional apparatus with a H_2/N_2 ratio in the feed of 1/9 and heating rate of $10\text{ }^\circ\text{C min}^{-1}$ from room temperature up to $950\text{ }^\circ\text{C}$.

Carbon deposits were characterized by temperature programmed oxidation (TPO), measuring the weight variation as function of the temperature in a thermogravimetric instrument (Shimadzu TGA 50). Post reaction samples of 0.015 g were used with air flow of $10\text{ cm}^3\text{ min}^{-1}$ and heating of $10\text{ }^\circ\text{C min}^{-1}$ from room temperature to $850\text{ }^\circ\text{C}$.

XPS analysis was performed with a Leybold Heraeus LHS10 spectrometer operating in FAT mode (50 eV pass energy), with $Al\text{ K}\alpha$ (1486.6 eV) radiation. A computer sequentially acquired the following regions: Ce (3d), Ni (2p), O (1s), C (1s), Zr (3d), and Al (2p). Reduction treatments *in situ* in a flowing H_2/N_2 mixture (2%vol) at $400\text{ }^\circ\text{C}$ for 2 h were carried out on samples previously treated in H_2 at $700\text{ }^\circ\text{C}$ for 1 h and exposed to air. Binding energy (BE) values, measured with an accuracy of $\pm 0.2\text{ eV}$, were referenced to C 1s at 285.0 eV , which always resulted in an Al (2p) peak at 74.5 eV (as for Al (2p) in Al_2O_3). Data analysis involved smoothing, X-ray satellite removal, non-linear Shirley-type background subtraction, curve fitting (mixed Gaussian–Lorentzian function by a least-square method) and peak area determination by integration of the appropriate signal after data analysis (Esca Tools 4.2 software, Surface Interface Inc., Mountain View, CA). Surface composition was determined by the peak area ratios using the empirically derived atomic sensitivity factors reported by Wagner [21].

Changes in the Ce 3d and Ni 2p signal shape on reduced samples were analyzed by a curve fitting procedure with Ce 3d

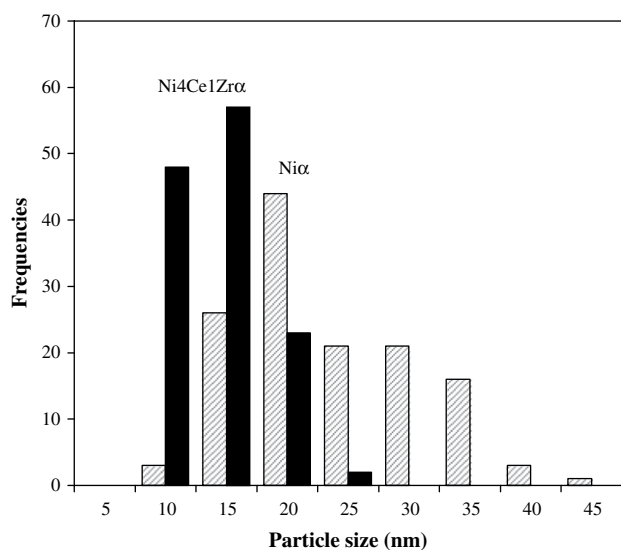


Fig. 1 – Particle size distribution determined by transmission electron microscopy (TEM).

and Ni 2p doublets endowed with fixed spectroscopic parameters, but using variable position, full width at half maximum (FWHM) and intensities.

3. Results and discussion

The commercial $\alpha\text{-Al}_2\text{O}_3$ used as base support presents a specific surface area around $10\text{ m}^2\text{ g}^{-1}$. The supports obtained by the addition of Ce and/or Zr oxides (1% and 5%) showed a larger number of surface active sites at the expense of a slight decrease of $\alpha\text{-Al}_2\text{O}_3$ surface area ($7\text{--}8\text{ m}^2\text{ g}^{-1}$). Since our results of characterization and catalytic activity are analogous for 1% and 5% of modifier oxides of the support, we only present results corresponding to 5% (Table 1).

In a previous work, we have demonstrated that the addition of Ce and Zr leads to $\alpha\text{-Al}_2\text{O}_3$ supports with patches of

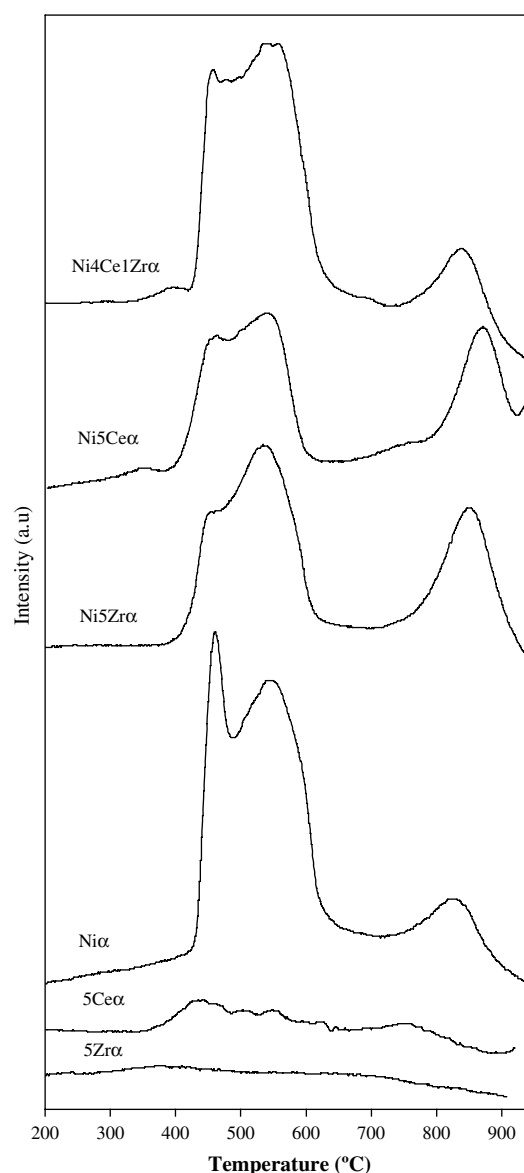


Fig. 2 – Temperature programmed reduction (TPR) profiles for $Ni\alpha$, $Ni_5Ce\alpha$, $Ni_4Ce_1Zr\alpha$, $Ni_5Zr\alpha$ catalysts and $5Ce\alpha$, $5Zr\alpha$ supports.

CeO₂ and ZrO₂ respectively, while in CeZr α composites, patches of mixed oxides type Ce_{1-x}Zr_xO₂ are formed. Particularly, with Ce:Zr = 4 ratio, the presence of mixed oxide of Ce_{0.8}Zr_{0.2}O₂ stoichiometry was proved [19].

The average diameter of nickel particle obtained by TEM indicates a slight decrease for modified supports (Table 1). Histograms representing metallic particle sizes (Fig. 1) show a more homogeneous distribution for systems with modified supports. Although they are scarcely dispersed systems, property supports based on α -Al₂O₃, the presence of modifier oxide on the support improves the Ni dispersion. It is also possible to appreciate that values of metallic dispersion obtained from TEM measurements (Brunelle equation [22]) are similar to those obtained by the method of hydrogen dynamic chemisorption.

Fig. 2 shows programmed temperature reduction profiles for catalysts under study. The H₂ consumption, Table 1, was calculated using CuO for calibration, and expressed as reduction degree estimation of samples, “Reducibility (%)”: [(H₂ amount consumed by TPR)/(theoretical amount of H₂ consumption for total reduction)] \times 100.

Three principal peaks of hydrogen consumption are observed in the Ni α catalyst at 463, 555 and 835 °C, which would indicate the presence of three phases, (i) NiO bulk, \sim 30% of the total reduced Ni, very weakly interacting with the support, (ii) mixed nickel and aluminum oxides, as majority species \sim 60%, with quite a strong interaction with the support, and (iii) NiAl₂O₄ species, \sim 10% of the total reduced Ni, strongly interacting with the support.

In the systems with modified supports, both H₂ consumption profiles and reducibility differ from the system based on Ni α ; the differences are more evident in the distribution of peaks than in the shift of temperatures. The intensity decrease of the signal at low temperature (\sim 450 °C), would indicate a decrease of the NiO bulk weakly interacting, whereas the increase of hydrogen consumption peaks at higher temperature could be related to NiO_x species strongly interacting with modifier oxides of the support (CeO₂, ZrO₂ and Ce_xZr_{1-x}O₂) [23].

Reduction of supported modifier oxides, 5Ce α and 5Zr α , show that the H₂ consumption is very low for 5Ce α and results negligible for 5Zr α ; consequently, changes in reduction profiles cannot be attributed to the reduction of supports [24].

Up to this moment, it is apparent that the strong Ni-modified support interaction is evidenced not only by the higher Ni dispersion on the support surface but also by the presence of NiO_x (Ni²⁺) species that are reduced at high temperatures and by the decrease of NiO bulk.

XPS analysis was used to determine the chemical composition of the catalyst surface and to better understand the nature of interactions between the dispersed Ni species and the supporting oxides. BE values for the different elements in the fresh samples (700 °C in air for 4 h) are consistent with the presence of Ni(II), Zr(IV) and Ce(IV). The O 1s peak is, in general, broad and complicated because of the non-equivalence of surface oxygen ions.

The occurrence of a strong interaction between ceria and zirconia in NiCeZr α specimen is evidenced by the decrease in the BE of Zr 3d_{5/2} (181.8 eV) with respect to the value for ZrO₂ (182.5 eV), as reported for ceria reach-side solid solution [25]. The relative dispersion of the various oxides on the alumina surface can be obtained from the atomic intensity ratios (Table 2). Comparing the bulk composition with the XPS derived surface composition, ceria–zirconia solid solution formation in NiCeZr α samples can be inferred from the agreement between bulk and surface nCe/nZr atomic ratios and from the increase of both nCe/nAl and nZr/nAl ratios. Ni α and Ni5Zr α catalysts exhibit Ni surface enrichment, whereas Ni5Ce α and Ni4Ce1Zr α reveal a homogeneous Ni surface distribution.

Typical changes of the Ni 2p region for both Ni α and Ni5Zr α catalysts after in-situ H₂ treatment are illustrated in Fig. 3 for Ni5Zr α , as an example. The Ni 2p spectra consisted of both Ni²⁺ and Ni⁰, suggesting that the applied reduction procedure did not result in a complete reduction of the nickel. Curve fitting of the Ni 2p region allowed determination of the contribution of Ni⁰ (853.2 \pm 0.2 eV) and Ni²⁺ species (main peak and associated satellite separated by 6.1 eV) (856.7 \pm 0.2 eV) as about 50% of the total intensity (Table 3). In

Table 2 – Bulk and surface atomic composition for catalysts after in situ treatment in flowing H₂/N₂ mixture.

Catalysts	nA/nB	(nNi/nCe)	(nNi/nZr)	(nNi/nAl)	(nCe/nZr)	(nCe/nAl)	(nZr/nAl)
Ni α	Bulk	–	–	0.018	–	–	–
	Fresh ^a	–	–	0.110	–	–	–
	H ₂ ^a	–	–	0.080	–	–	–
Ni5Zr α	Bulk	–	0.840	0.018	–	–	0.022
	Fresh ^a	–	1.650	0.103	–	–	0.065
	H ₂ ^a	–	1.210	0.075	–	–	0.060
Ni5Ce α	Bulk	1.17	–	0.018	–	0.015	–
	Fresh ^a	0.91	–	0.091	–	0.105	–
	H ₂ ^a	0.80	–	0.090	–	0.110	–
Ni4Ce1Zr α	Bulk	1.46	4.20	0.018	2.86	0.012	0.004
	Fresh ^a	1.24	4.90	0.127	3.20	0.103	0.030
	H ₂ ^a	1.10	4.80	0.130	3.60	0.140	0.026

Surface atomic ratios were calculated according to the equation: nA/nB = (I_A/S_A)/(I_B/S_B), were S_A and S_B refer to the empirically derived sensitivity factors [21].

a Flowing H₂/N₂ mixture.

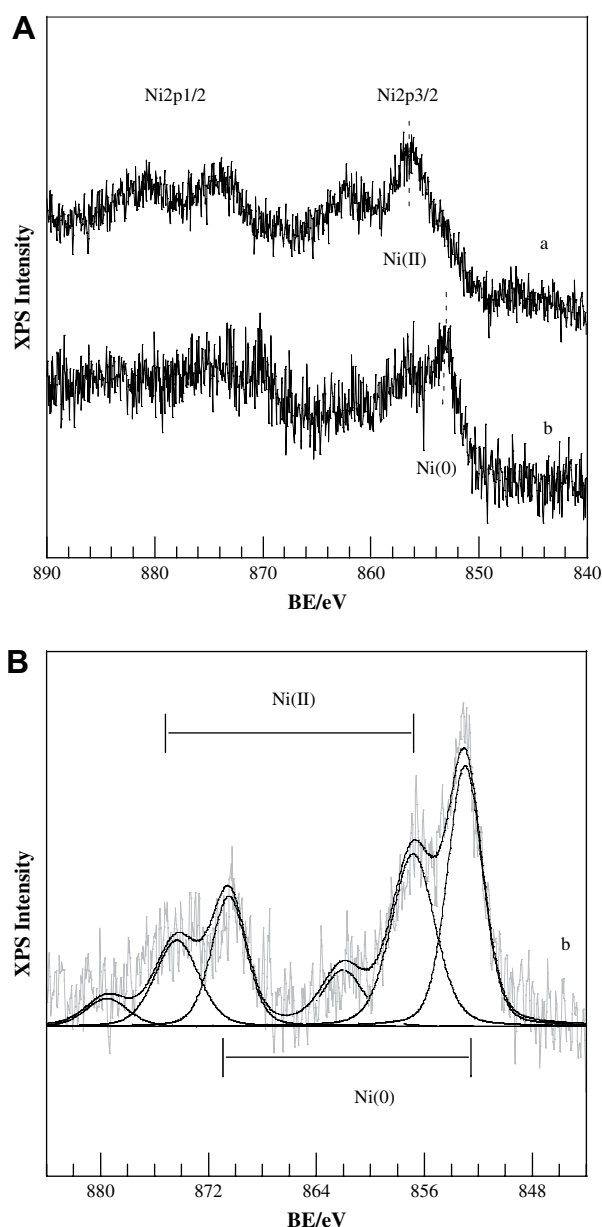


Fig. 3 – Ni 2p spectra of Ni5Zr α sample. (A) Curve a, fresh sample (700 °C in air for 4 h); curve b, reduced sample after in situ treatment in H₂. (B) Ni 2p_{3/2} signal shape analysis of spectrum b.

addition the reduction treatment induced Ni species, clustering as indicated by the decrease of nNi/nAl and nNi/nZr ratios (Table 2). For Ni5Ce α and Ni4Ce1Zr α catalysts the complex Ce 3d and Ni 2p region (Figs. 4 and 5, respectively), collectively resolved by curve fitting, contained both Ni⁰ (853.2 ± 0.2 eV) and Ni²⁺ species (856.7 ± 0.2 eV). The fraction of Ni⁰ is higher in Ni4Ce1Zr α than in Ni5Ce α (Table 3), but no variation of Ni distribution on the surface is detected (Table 2).

The Ce 3d region shows complex but distinct features arising from final-state effects and from the presence of both Ce⁴⁺ and Ce³⁺ oxidation states.

For Ce⁴⁺ the Ce 3d_{5/2} and Ce 3d_{3/2} lines (separated by about 18.5 eV) are characterized by three contributions denoted as v,

Table 3 – XPS results from curve fitting of Ce 3d_{5/2} and Ni 2p_{3/2} regions after in situ H₂ reduction.

Catalyst	Ni 2p _{3/2} (eV)	Ce 3d _{5/2} (eV)
Ni α	853.3 (Ni ²⁺ , 55%)	–
	856.9 (Ni ⁰ , 45%)	–
Ni5Zr α	853.2 (Ni ²⁺ , 48%)	–
	856.6 (Ni ⁰ , 52%)	–
Ni5Ce α	853.2 (Ni ²⁺ , 50%)	883.2 (v)
	856.7 (Ni ⁰ , 50%)	885.9 (v')
Ni4Ce1Zr α	853.3 (Ni ²⁺ , 75%)	916.8 (u''', 9.5%)
	856.8 (Ni ⁰ , 25%)	883.0 (v)
		885.3 (v')
		916.8 (u''', 5.2%)

In parentheses: chemical state and corresponding reduction degree.

v', v''' and u, u'', u''', respectively [26]. The presence of Ce³⁺ introduces in addition two contributions denoted as v₀, v' and u₀, u'. Because the u''' peak arises exclusively from Ce⁴⁺, it can be used as quantitative measure of Ce⁴⁺ amount. The integrated area of the u''' component with respect to the total Ce 3d area should constitute around 14% of total integral intensity [27]. Cerium is in reducible form in both Ni5Ce α and Ni4Ce1Zr α catalysts. Comparing the contribution of the u''' component revealed in Ni5Ce α and Ni4Ce1Zr α samples (Table 3), it is apparent that the Ni4Ce1Zr α shows a higher reducibility than Ni5Ce α . In both samples, however, the surface compositions resemble that of bulk.

The behavior of each catalyst, evaluated facing the different reforming reactions (see experimental section), indicates that the reactivity trend POM \approx MR > DR \approx SR does not change by support modifications (Fig. 6).

Similar reaction rates for SR and DR were found as already reported [28]. In MR reaction, the replacement of H₂O by O₂ in the reaction mixture (CH₄/O₂/H₂O = 2/1/1) provokes a marked increase in catalytic activity. This could be explained by the fast methane combustion with oxygen present in the feed, generating a temperature increase that produces the increase in the reforming rate [23,29–31].

The H₂/CO ratio in the synthesis gas results is higher than the stoichiometric value of each reaction: SR \sim 3–3.5, POM \sim 2–2.5, and MR \sim 2–3, which suggests the important contribution of WGS reaction.

With respect to differences among catalysts, catalysts based on modified supports showed higher activity in all reactions, in agreement with the higher concentration of active sites on the surface (Fig. 6). In DR reaction, higher differences in activity are noticed by the support effect, in agreement with some authors who established the participation of Ce and Zr oxides in CO₂ chemisorption [32–34]. Among composites, the Ni4Ce1Zr α sample presented the highest activity, evidencing the importance of Ce_{0.8}Zr_{0.2}O₂ on the support surface in active phase generation.

We performed a deep analysis of catalyst stability against sintering and carbon deposition, which are critical properties of nickel catalysts. Sintering is a thermal degradation process difficult to prevent production of, generally, irreversible deactivation. Ferretti et al. demonstrated that the water steam in the feed produces a marked metallic area decrease in

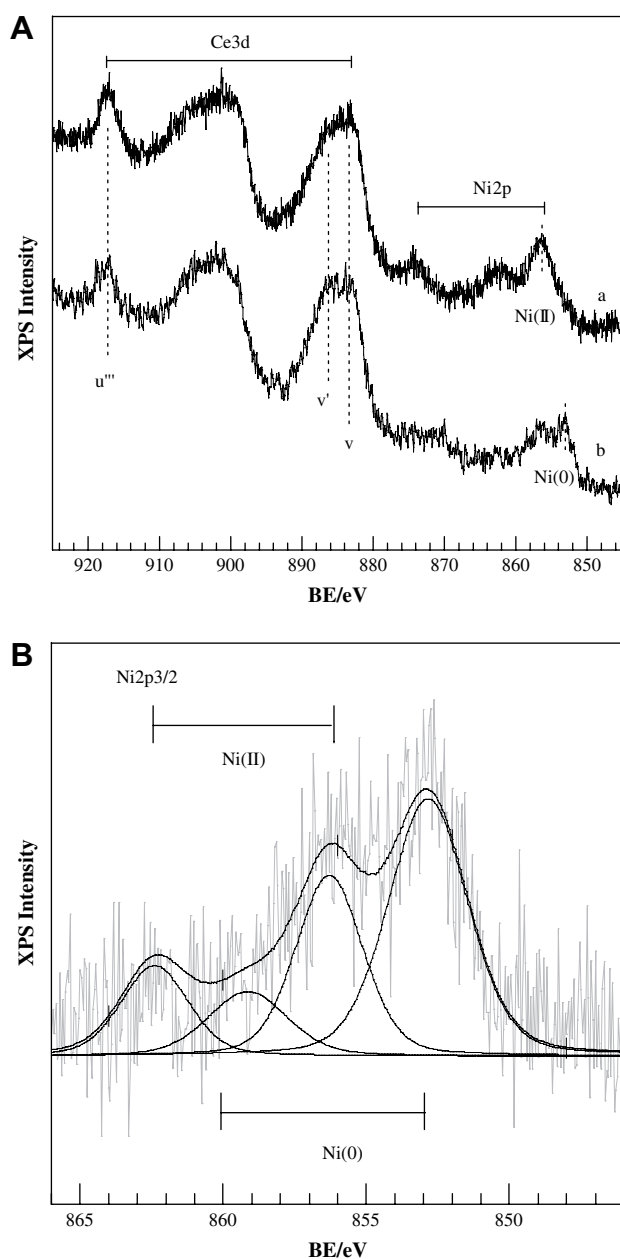


Fig. 4 – Ce 3d and Ni 2p spectra of Ni₅Ce_α catalyst. (A) Curve a, fresh sample (700 °C in air for 4 h); curve b, reduced sample after in situ treatment in H₂. (B) Ni 2p_{3/2} signal shape analysis of spectrum b.

supported nickel catalysts [35]. Among all reforming processes investigated in this work, the SR reaction allows the most favorable conditions for sintering.

Deactivation by carbon deposition is also critical. The formation of a carbon film covering the active site as well as the formation of carbon filaments or whiskers represents serious operational problems. Among all reactions studied, reforming with CO₂ (DR) is the one that mostly favors the deactivation by carbon deposition, because of the high carbon contribution in the feed and the high temperature required. Besides, the thermodynamic analysis indicates that for reaction temperatures in the range 550 and 700 °C, the carbon

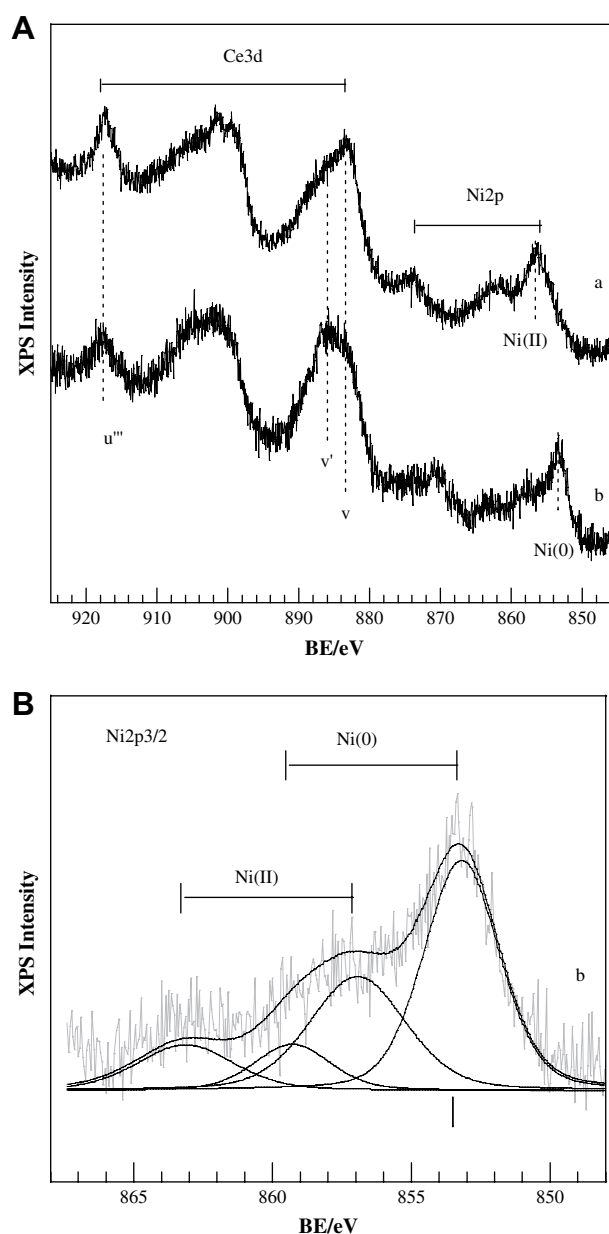


Fig. 5 – Ce 3d and Ni 2p spectra of Ni₄Ce₁Zr_α catalyst. (A) Curve a, fresh sample (700 °C in air for 4 h); curve b, reduced sample after in situ treatment in H₂. (B) Ni 2p_{3/2} signal shape analysis of spectrum b.

deposition could come from methane cracking reaction as well as from “Boudouard” reaction [36].

In order to evaluate the resistance to the two principal deactivation sources, sintering and carbon deposition, stability tests were applied in two different deactivating conditions. In the first test, Test (A), SR reaction is performed with intervals of steam flow at 800 °C (for more details see Section 2). The results (Table 4) indicate the high deactivation degree for Ni_α and Ni₅Zr_α, with a_{CH_4} equal to 0.35 and 0.15, respectively.

Sintering resulted the prevailing source in the deactivation, as evidenced by the mean post-reaction particle diameter (d_{va}) and carbon deposited (%wt/wt C) (Table 4): carbon content

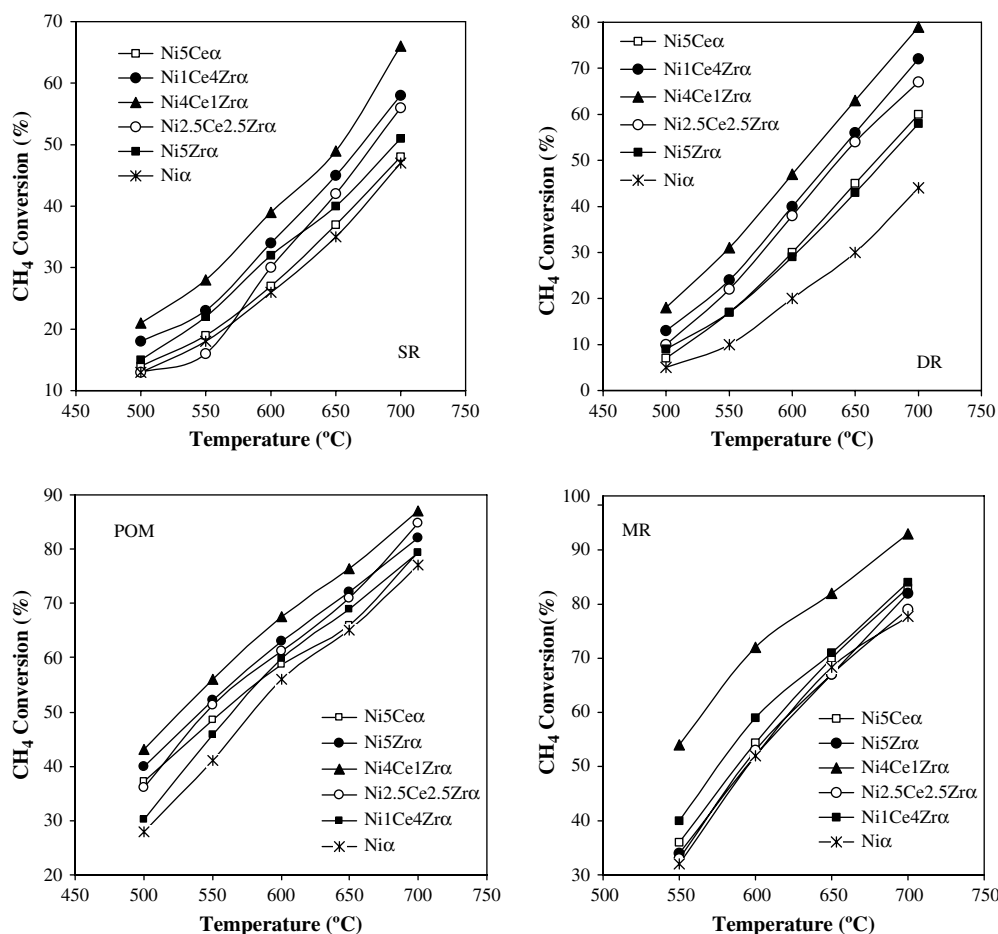


Fig. 6 – Methane conversions as function of the temperature in reforming reactions: steam reforming (SR), partial oxidation (POM), dry reforming (DR) and mixed reforming (MR). GHSV = $3 \times 10^5 \text{ cm}^3 \text{ h}^{-1} \text{ g}^{-1}$.

was very low (less than 0.35% wt/wt), whereas the increase of metallic particle size was significant in catalysts with the higher deactivation (60% and 47%). In this way, Niα and Ni5Zrα systems resulted in less resistance to sintering. In Ni5Zrα,

besides the increase of metal particle size, the zirconia migration on metallic particles covering the active sites was determined by XPS, in agreement with previous findings [37].

The composite systems show the lowest deactivation degree (a_{CH_4} : 0.74–0.84). The presence of mixed oxides of the type $\text{Ce}_x\text{Zr}_{1-x}\text{O}_2$ improves noticeably the thermal stability of the catalyst, as indicated by other authors [23].

The second stability test, Test (B), carried out under conditions favoring carbon deposition (Fig. 7), indicates that all the catalysts based on modified alumina are more stable than the Niα catalysts. Catalysts modified with Ce and those containing composites show the best improvements. The carbon content on Ni4Ce1Zrα, Ni2.5Ce2.5Zrα and Ni1Ce4Zrα samples (<0.6% wt/wt C) was an order of magnitude lower than Niα catalysts (6.9% wt/wt C). TEM micrographs show “whiskers” type carbon filaments and an increase of particle size in post-reaction samples of about 24–27% (Fig. 8). These results allow one to conclude that improvements in stability are produced by the low carbon deposition.

Our results can be analyzed according to the reaction mechanisms proposed by Qin et al. [38] and Rostrup-Nielsen [39] that allow an explanation of the significant differences in activity and stability depending on the support type. Scheme 1 shows the steps corresponding to methane activation (from 1 to 2),

Table 4 – Results obtained after sintering process.

Catalyst	Test A (sintering)			Test B (carbon deposition)		
	a_{CH_4} (24 h)	C (%wt/wt) (TPO/TGA)	Particle size increase (%) (TEM)	a_{CH_4} (70 h)	C (%wt/wt) (TPO/TGA)	Particle size increase (%) (TEM)
Niα	0.35	0.33	60	0.24	6.9	40
Ni5Zrα	0.15	0.25	47	0.44	1.8	32
Ni4Ce1Zrα	0.84	0.10	25	0.86	0.3	24
Ni2.5Ce2.5Zrα	0.80	0.15	28	0.78	0.6	27
Ni1Ce4Zrα	0.74	0.12	30	0.70	0.4	27
Ni5Ceα	0.65	0.22	37	0.58	2.1	29

Particle size increase %: $[(d_{\text{TEM post-reaction}} - d_{\text{TEM fresh}}) / d_{\text{TEM fresh}} \times 100]$.

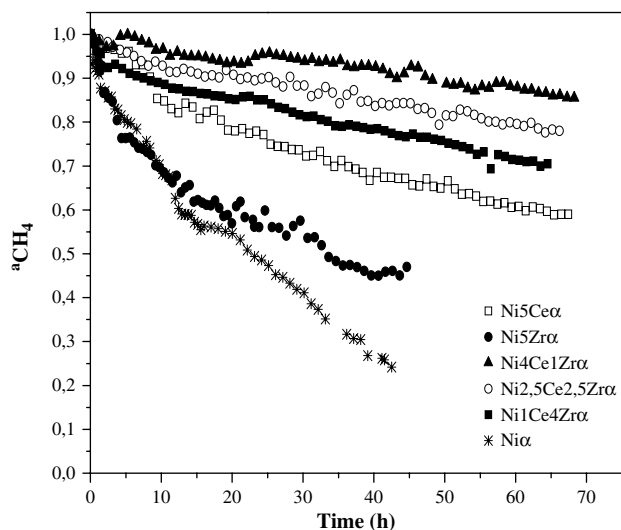


Fig. 7 – Deactivation tests of the studied catalysts. Reaction: dry reforming. Feed flow rate $130 \text{ cm}^3 \text{ min}^{-1}$ ($\text{N}_2/\text{CH}_4/\text{CO}_2 = 14/2/2$), $T = 700 \text{ }^\circ\text{C}$, $a_{\text{CH}_4} = \text{XCH}_4(t)/\text{XCH}_4(i)$.

generation of adsorbed oxygen on surface sites, O-S (from 3 to 5), and formation of CO and H₂ (from 6 to 8). By assuming that the global activity results by the activation rate of CH₄ and by the reaction between species CH_x-S and O-S (stage (6)), the difference in the rates between reactions POM, MR and DR would be produced by the higher amount of sites O-S in the POM and MR (stage (4) versus stage (3)) than in DR.

The small contribution of O-S in DR could be responsible for the lower reaction rate, allowing the development of

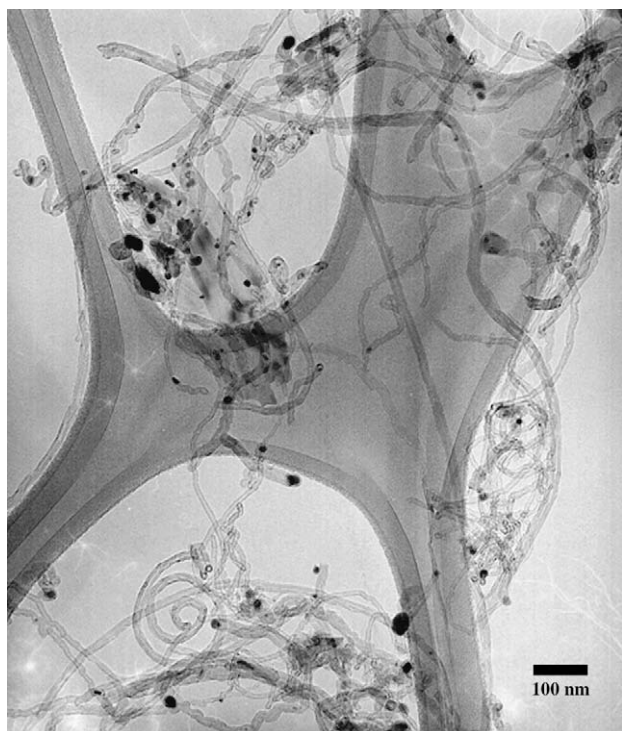


Fig. 8 – TEM micrographs of Ni4Ce1Zrα catalyst, after DR deactivation test at 700 °C.

1. $\text{CH}_x + 2\text{S} \rightarrow \text{CH}_{x-1}\text{-S} + \text{H-S} \quad (2 < x < 4)$
2. $\text{CH-S} + \text{S} \rightarrow \text{C-S} + \text{H-S}$
3. $\text{CO}_2 + 2\text{S} \rightarrow \text{CO-S} + \text{O-S}$
4. $\text{O}_2 + 2\text{S} \rightarrow 2\text{O-S}$
5. $\text{H}_2\text{O} + 3\text{S} \rightarrow \text{O-S} + 2\text{H-S}$
6. $\text{CH}_x\text{-S} + \text{O-S} + (x-1)\text{S} \rightarrow \text{CO-S} + x\text{H-S}$
7. $\text{CO-S} \rightarrow \text{CO} + \text{S}$
8. $2\text{H-S} \rightarrow \text{H}_2 + 2\text{S}$

Scheme 1 – Reaction scheme to obtain synthesis gas [38].

intermediate species that lead to higher carbon formation. In addition, the activity improvement in DR measured on composites could be due to the role played by the support in step dealing with O-S formation.

With respect to stability, the higher availability of adsorbed O-S species allows the CO production with lower carbon formation. Our results indicate that the provision of these O-S sites by the support property follows the order: Ni4Ce1Zrα > Ni1Ce4Zrα, Ni2.5Ce2.5Zrα > Ni5Ceα > Ni5Zrα > Niα. The same stability order is established for catalysts with 1% wt/wt of modifier oxides.

4. Conclusions

The present study indicates that the addition of small amounts of CeO₂ and ZrO₂ to α-Al₂O₃ allows procurement of a support with patches of Ce_xZr_{1-x}O₂ mixed oxide on the surface. This support, improving the Ni dispersion and the metal particle reducibility, leads to catalysts with a high activity for all methane reforming reactions in the temperature range investigated (450–700 °C). The improvement is more marked for reactions involving CO₂ and O₂ as reagent (DR and POM) due to the contribution of the support in generating reaction steps with surface adsorbed oxygen species. As for stability, the Ce_{0.8}Zr_{1-x}O₂ patches provide the highest benefits not only by the high oxygen storage capacity (OSC) which prevents the carbon deposition but also by the metal-support interaction that prevents deactivation by sintering.

Acknowledgments

The present work has been financed by CONICET (PIP 02738) and ANPCYT-FONCYT (14-14122), Argentina.

REFERENCES

- [1] Dias JAC, Assaf JM. Autoreduction of promoted Ni/γ-Al₂O₃ during autothermal reforming of methane. *Journal of Power Sources* 2005;139(1-2):176–81.

- [2] Ferreira-Aparicio P, Benito MJ, Sanz JL. New trends in reforming technologies: from hydrogen industrial plants to multifuel microreformers. *Catalysis Reviews: Science and Engineering* 2005;47(4):491–588.
- [3] Cacciola G, Antonucci V, Freni S. Technology up date and new strategies on fuel cells. *Journal of Power Sources* 2001; 100(1-2):67–79.
- [4] Armor JN. The multiple roles for catalysis in the production of H₂. *Applied Catalysis A: General* 1999;176(2):159–76.
- [5] Navarro RM, Peña MA, Fierro LG. Hydrogen production reactions from carbon feedstocks: fossil fuels and biomass. *Chemical Review* 2007;107:3952–91.
- [6] Rostrup-Nielsen JR, Sehested J, Nørskov JK. Hydrogen and synthesis gas by steam and CO₂ reforming. *Advances in Catalysis* 2002;47:65–139.
- [7] Benggaard HS, Nørskov JK, Sehested J, Clausen BS, Nielsen LP, Molenbroek M, et al. Steam reforming and graphite formation on Ni catalysts. *Journal of Catalysis* 2002;209(2):365–84.
- [8] Pompeo F, Nichio NN, Ferretti OA, Resasco DE. Study of Ni catalysts on different supports to obtain synthesis gas. *International Journal of Hydrogen Energy* 2005;30:1399–405.
- [9] Nichio NN, Casella ML, Ponzi EN, Ferretti OA. Ni/Al₂O₃ catalysts for syngas obtention via reforming with O₂ and/or CO₂. *Studies in Surface Science and Catalysis* 1998;119:723–8.
- [10] Pompeo F, Nichio NN, González MG, Montes M. Characterization of Ni/SiO₂ and Ni/Li-SiO₂ catalysts for methane dry reforming. *Catalysis Today* 2005;107–108:856–62.
- [11] Dutta G, Waghmare UV, Baidya T, Hegde MS, Priolkar KR, Sarode PR. Reducibility of Ce_{1-x}Zr_xO₂: origin of enhanced oxygen storage capacity. *Catalysis Letters* 2006;108(3-4):165–72.
- [12] Roh HS, Potdar HS, Jun KW. Carbon dioxide reforming of methane over co-precipitated Ni-CeO₂, Ni-ZrO₂ and Ni-Ce-ZrO₂ catalysts. *Catalysis Today* 2004;93–95:39–44.
- [13] Wang S, Lu GQ. Role of CeO₂ in Ni/CeO₂-Al₂O₃ catalysts for carbon dioxide reforming of methane. *Applied Catalysis B: Environmental* 1998;19(3-4):267–77.
- [14] Roh HS, Jun KW, Park SE. Methane-reforming reactions over Ni/Ce-ZrO₂/θ-Al₂O₃ catalysts. *Applied Catalysis A: General* 2003;251(2):275–83.
- [15] Oh YS, Roh HS, Jun KW, Baek YS. A highly active catalyst, Ni/Ce-ZrO₂/θ-Al₂O₃, for on-site H₂ generation by steam methane reforming: pretreatment effect. *International Journal of Hydrogen Energy* 2003;28:1387–92.
- [16] Laosiripojana N, Assabumrungrat S. Methane steam reforming over Ni/Ce-ZrO₂ catalyst: Influences of Ce-ZrO₂ support on reactivity, resistance toward carbon formation, and intrinsic reaction kinetics. *Applied Catalysis A: General* 2005;290(1-2):200–11.
- [17] Roh HS, Jun KW, Dong WS, Chang JS, Park SE, Joe YI. Highly active and stable Ni/Ce-ZrO₂ catalyst for H₂ production from methane. *Journal of Molecular Catalysis A: Chemical* 2002; 181(1-2):137–42.
- [18] Gao J, Guo J, Liang D, Hou Z, Fei J, Zheng X. Production of syngas via autothermal reforming of methane in a fluidized-bed reactor over the combined CeO₂-ZrO₂/SiO₂ supported Ni catalysts. *International Journal of Hydrogen Energy* 2008; 33(20):5493–500.
- [19] Pompeo F, Gazzoli D, Nichio NN. Characterization of α-Al₂O₃ supports modified with CeO₂ and ZrO₂. *Materials Letters* 2009;63:477–9.
- [20] Froment GF, Bischoff KB. *Chemical reactor analysis and design*. New York: John Wiley and Sons; 1979.
- [21] Wagner CD, Davis LE, Zeller MV, Taylor JA, Raymond RH, Gale LH. Empirical atomic sensitivity factors for quantitative analysis by electron spectroscopy for chemical analysis. *Surface and Interface Analysis* 1981;3(5):191–234.
- [22] Brunelle JP, Sugier A, Le Page JF. Active centers of platinum-silica catalysts in hydrogenolysis and isomerization of n-pentane. *Journal of Catalysis* 1976;43(1-3):273–91.
- [23] Roh HS, Jun KW, Dong WS, Park SE, Baek YS. Highly stable Ni catalyst supported on Ce-ZrO₂ for oxy-steam reforming of methane. *Catalysis Letters* 2001;74:31–6.
- [24] Roh HS, Jun KW, Baek SC, Park SE. A highly active and stable catalyst for carbon dioxide reforming of methane: Ni/Ce-ZrO₂/θ-Al₂O₃. *Catalysis Letters* 2002;81:147–51.
- [25] Nelson AE, Schulz KH. Surface chemistry and microstructural analysis of Ce_xZr_{1-x}O_{2-y} model catalyst surfaces. *Applied Surface Science* 2003;210(3-4):206–21.
- [26] Rama Rao MV, Shripathi T. Photoelectron spectroscopic study of X-ray induced reduction of CeO₂. *Journal of Electron Spectroscopy and Related Phenomena* 1997;87(2): 121–6.
- [27] Shyu JZ, Otto K, Watkins WLH, Graham GW, Belitz RK, Gandhi HS. Characterization of Pd/γ-alumina catalysts containing ceria. *Journal of Catalysis* 1988;114(1):23–33.
- [28] Xu J, Froment GF. Methane steam reforming, methanation and water-gas shift: I. Intrinsic kinetics. *AIChE Journal* 1989; 35:88–96.
- [29] Ayabe S, Omoto H, Utaka T, Kikuchi R, Sasaki K, Teraoka Y, Eguchi K. Catalytic autothermal reforming of methane and propane over supported metal catalysts. *Applied Catalysis A* 2003;241:261–9.
- [30] Takeguchi T, Furukawa SN, Inoue M, Eguchi K. Autothermal reforming of methane over Ni catalysts supported over CaO-CeO₂-ZrO₂ solid solution. *Applied Catalysis A* 2003;240: 223–33.
- [31] Souza MMVM, Schmal M. Autothermal reforming of methane over Pt/ZrO₂/Al₂O₃ catalysts. *Applied Catalysis A* 2005;281:19–24.
- [32] Stagg-Williams SM, Noronha FB, Fendley G, Resasco DE. CO₂ reforming of CH₄ over Pt/ZrO₂ catalysts promoted with La and Ce oxides. *Journal of Catalysis* 2000;194(2):240–9.
- [33] Xu BQ, Wei JM, Yu YT, Li JL, Zhu QM. Carbon dioxide reforming of methane over nanocomposite Ni/ZrO₂ catalysts. *Topics in Catalysis* 2003;22(1-2):77–85.
- [34] Wei JM, Xu BQ, Li JL, Cheng ZX, Zhu QM. Highly active and stable Ni/ZrO₂ catalyst for syngas production by CO₂ reforming of methane. *Applied Catalysis A: General* 2000; 196(2):1167–72.
- [35] Ferretti OA, Marecot P, Demicheli MC, Gonzalez MG, Duprez D, Barbier J. Etude de la stabilité et de l'empoisonement par le soufre de catalyseur de vaporeformage NiAlumine. *Bulletin de la Société Chimique de France* 1990;127:347.
- [36] Wang S, Lu GQ, Millar GJ. Carbon dioxide reforming of methane to produce synthesis gas over metal-supported catalysts: state of the art. *Energy Fuels* 1996;10(4):896–904.
- [37] Bulgakov NN, Sadykov VA, Lunin VV, Kemnitz E. Lattice defects and oxygen absorption/migration in ceria/ceria-zirconia solid solutions: analysis by semiempirical interacting bonds method. *Reaction Kinetics and Catalysis Letters* 2002;76(1):103–10.
- [38] Qin D, Lapszewicz J, Jiang X. Comparison of partial oxidation and steam-CO₂ mixed reforming of CH₄ to Syngas on MgO-supported metals. *Journal of Catalysis* 1996;159(1):140–9.
- [39] Rostrup-Nielsen JR, Alstrup I. Innovation and science in the process industry: Steam reforming and hydrogenolysis. *Catalysis Today* 1999;53(3):311–6.